RSC Advances




ROYAL SOCIETY OF CHEMISTRY

www.rsc.org/advances

# Morphological diagram of nucleating agent/poly(ε-caprolatone) and in-situ barriering strategy

Siqi Wu, Rui Han, Min Nie*, Qi Wang

Address: State Key Laboratory of Polymer Materials Engineering, Polymer Research Institute of Sichuan University, Chengdu 610065, China

Email: poly.nie@gmail.com

Fax: +86-28-85402465

Tel: +86-28-85405133

Abstract: This paper constructed the temperature/composition morphological diagram of nucleating agent/poly(ε-caprolatone) blends to direct in-situ formation of flake nucleating agents with excellent capacity of promoting the interfacial interaction, which were well-suited choices for barrier polymers.

Polymers become widely used in packaging and protective applications, but almost polymers exhibit an inherent permeability to gas, water and other small molecules[1]. Therefore, barrier polymers have gained world-wide attention. By far, many technologies have been developed to improve barrier properties of polymer materials[2-5], such as vacuum-deposited coating, lamination or co-extrusion with high-barrier polymer, layer-by-layer assembly. Additionally, when inert nonporous fillers are incorporated into polymer matrix, the permeating molecules must circumvent fillers in a tortuous path, rather than in a straight line path, to pass through polymer matrix, resulting in an extended travelling pathway[6]. Introduction of the impermeable filler has been proved to a facile route for the enhanced barrier properties and the ameliorations are strongly dependent on the filler morphology[7]. Based on the Nielsen model, the flake fillers of high lateral dimension are the most promising materials in gas- or liquid-barrier applications[8]. Kim only used 3wt% layered graphene as filler in polyurethane to achieve 90% decrease in nitrogen permeation[9]. Nevertheless, the successful applications of the layered fillers require the uniform dispersion and strong interface interaction with polymer matrix. This is often unavailable and thus the prerequisite is chemical modification of the fillers.

Nucleating agents have favorable matching lattice with polymer to break down nucleation barrier of polymer, so the nucleation is much more favored on their surface[10]. It is evident that the interfacial crystallization can realize the enhancement of interfacial interaction in semicrystalline polymer/filler composites[11]. Recently, some kinds of novel supermolecular nucleating agents are reported to dissolve in the polymer melts and recrystallize upon cooling. Through this dissolution-recrystallization process, the nucleating agents can disperse homogeneously in polymer matrix, even if the initial dispersion is unsatisfactory[12, 13]. More notably, the nucleating agent can self-assemble into different topological structure, such as dot, fibrous, dendric morphology[14-16]. Flake nucleating agents induced via regulation of the self-assembly behaviors are expected to construct barrier layer with uniform dispersion in polymer matrix, but the formation mechanism on flake nucleating agents is not mapped yet. Accordingly, comprehensive understanding on solubility and self-assembly of nucleating agent is very important. In this paper, TMB-5(NAs), well-known aryl amide-based nucleating agent, which could be driven by intermolecular hydrogen bonding to self-assemble in polymer melts or solution[17, 18], was selected as a model and its morphological manipulation in an environmentally friendly biomaterial poly(ε-caprolatone)(PCL) was performed by adjusting the temperature and concentration of NAs, and thus a morphological diagram on the temperature and concentration was constructed, providing a theoretical and practical guide to achieve in-situ formation of flake nucleating agents and finally barrier polymer. [Detailed descriptions of the related materials, sample preparation and

characterizations are provided in ESI]

The dissolution and recrystallization behaviors of NAs in PCL matrix were determined by optical microscope with hot stage. Figure 1 showed typical optical micrographs for PCL/NAs blends during the heating and cooling processes. Clearly, with the increasing temperature, the PCL crystals first melted, then the NAs gradually dissolved into the molten PCL. Very interesting, during the cooling process from different molten temperature, the morphologies of NAs could be manipulated, i.e., dot, fiber and flake. Based on the dissolution and solidification temperatures of NAs(see Figure 1S in ESI), one observed that the complete dissolution temperature was higher than the formed temperatures of fiber-like NAs and exhibited almost same as that where flake-like NAs were generated. It indicated that the key factor affecting the morphologies of NAs was the dissolution state. Specifically, when NAs didn't dissolve into the polymer melts, the morphology of NAs remained unchanged. At high melting temperature, NAs partially dissolved in PCL matrix and in the subsequent cooling process, the dissolved NAs preferred to grow along the long axis of these undissolved ones, forming the fiber. As the temperatures increased further, the solubility of NAs became high and only a few NAs as nuclei were left in the melt. In this case, the lateral growth was observed besides the longitude growth. As shown in Fig. 1f, the breadth of the fiber became bigger and the two-dimensional flake nucleating agent was generated. To the best of our knowledge, it is investigated for the first time that nucleating agent self-assembled into flake structures in the polymer matrix, different from the three-dimensional dendritic structures in polypropylene[17, 19].

This can be ascribed to polar difference of the two polymer ones. NAs containing amide groups was polar while PP was nonpolar, so upon cooling, the dissolved NAs might separate quickly from the nonpolar PP melts, lead to fast nucleation and growth with the result of dendrite-like structure. On the contrary, in polar PCL melts, NAs dissolved out slower and the crystals grew synchronously along the longitude and lateral directions. As a result, flake structures were generated. However, the underlying mechanism for different morphologies of the nucleating agents still remained unclear.

Further, the morphological evolution of NAs upon cooling as a function of the additive concentration was investigated and the temperature/composition morphological diagram was constructed. As shown in Fig. 2, there were three diverse morphological regions, which were separated by red solid line represented the formed temperature of fiber NAs and blue dash line was corresponded to the critical formed temperature of flake structure. Obviously, the solubility and the final morphology of NAs in PCL melts was closely related to the melting temperature and the concentration of NAs. At the low melting temperature, NAs still remain the original particles. However, when the concentration of NAs was low, even if NAs dissolved into PCL melts at high melting temperature, no morphological transformation was identified upon cooling because there were not enough NAs available for the growth of fiber or flake. Therefore, dot-like NAs appeared in region I. Region II was divided into two parts: one was located at the intermediate concentration, where NAs was consumed completely due to preferential growth of the fiber; the other was at high

concentration and the medium temperature, in which the low solubility of NAs dictated only the formation of the fiber. With the rising concentration and melting temperature(region III), sufficient dissolved NAs could grow along the longitude and lateral direction so flake nucleating agents were achieved. Moreover, it is worth mentioning that although the formed temperature for flake morphology was high compared to the melting temperature of PCL, it could not affect the properties of PCL. [TGA and DSC results are described in ESI]

As a good barrier materials, the flake nucleating agents are required to possess excellent compatible interface with polymer. Interfacial crystallization is a versatile approach to promote the interfacial interaction. It is acknowledged that crystallization temperature(Tc) can be used as a criterion to evaluate the nucleation efficiency of nucleating agent. The higher the Tc, the lower the nucleation barrier. When the difference between the crystallization temperature of the nucleated polymer and pure polymer is bigger than 6.5$^{o}$C, the nucleating agent is considered as high efficient one[20]. As shown in Fig. 3a, with the presence of NAs, the crystallization temperature of PCL did rise significantly. At the concentration of 0.7%, the crystallization increased from 25.9$^{o}$C of pure PCL to 36.9 °C and remained constant at higher NAs concentration. It indicated NAs was a good nucleating agent for PCL, which was contributed to the perfect lattice matching between the two materials. [XRD results are described in ESI] Therefore, it seems that NAs can provides the large surface of active nucleation sites for PCL crystallization. The direct observations on the epitaxial crystallization of PCL were presented in Fig. 3b-d. Distinctly, compared to

homogenous nucleation of pure PCL(Fig.3b), crystallization of PCL firstly started on the surface of NAs, where crystal nuclei densely located, indicating the strong heterogeneous nucleation ability of NAs. The transcrystalline grew on the NAs was favorable to the increased interfacial interaction between PCL and NAs. Herein, the other key issue of the flake material used in barrier polymer was solved successfully.

In summary, this paper presented a novel strategy to prepare high-barrier polymer via morphological manipulation of flake nucleating agent in PCL melts and construct the temperature/composition diagram. Since NAs exhibited high nucleation efficiency for PCL, the polymer preferred to epitaxially crystallize on the surface of NAs and the excellent interfacial interaction was achieved. Expectedly, the flake nucleating agent can behave as good barrier layer in polymer materials, providing an easy but effective solution for preparation of high-barrier materials.

This work is financiered by the National Natural Science Foundation of China (51421061).

Notes and references

1. J. Lange and Y. Wyser, *Packag Technol Sci*, 2003, **16**, 149.
2. J. P. Cerisuelo, R. Gavara and P. Hernandez-Munoz, *J Membrane Sci*, 2015, **482**, 92.
3. J. J. Decker, K. P. Meyers, D. R. Paul, D. A. Schiraldi, A. Hiltner and S. Nazarenko, *Polymer*, 2015, **61**, 42.
4. M. A. Priolo, K. M. Holder, T. Guin and J. C. Grunlan, *Macromol Rapid Comm*, 2015, **36**, 866.

5. L. Xie, H. Xu, J.B. Chen, Z.J. Zhang, B. S. Hsiao, G.J. Zhong, J. Chen and Z.M. Li, *ACS Appl Mater Interf*, 2015, **7**, 8023.

6. T. V. Duncan, *J Colloid Interf Sci*, 2011, **363**, 1.

7. R. K. Bharadwaj, *Macromolecules*, 2001, **34**, 9189.

8. T. Kim, J. H. Kang, S. J. Yang, S. J. Sung, Y. S. Kim and C. R. Park, *Energy Environ Sci*, 2014, **7**, 3403.

9. H. Kim, Y. Miura and C. W. Macosko, *Chem Mater*, 2010, **22**, 3441.

10. M. Blomenhofer, S. Ganzleben, D. Hanft, H.-W. Schmidt, M. Kristiansen, P. Smith, K. Stoll, D. Mäder and K. Hoffmann, *Macromolecules*, 2005, **38**, 3688.

11. N. Ning, S. Fu, W. Zhang, F. Chen, K. Wang, H. Deng, Q. Zhang and Q. Fu, *Prog Polym Sci*, 2012, **37**, 1425.

12. D. Libster, A. Aserin and N. Garti, *Polym Adv Tech*, 2007, **18**, 685.

13. A. Thierry, B. Fillon, C. Straupé, B. Lotz and J. C. Wittmann, in *Solidification Processes in Polymers*, eds. J. F. Janssson and U. W. Gedde, Steinkopff, 1992, 87, 28.

14. M. Kristiansen, M. Werner, T. Tervoort, P. Smith, M. Blomenhofer and H. W. Schmidt, *Macromolecules*, 2003, **36**, 5150.

15. N. D. Treat, J. A. Nekuda Malik, O. Reid, L. Yu, C. G. Shuttle, G. Rumbles, C. J. Hawker, M. L. Chabinyc, P. Smith and N. Stingelin, *Nat Mater*, 2013, **12**, 628.

16. J. Varga and A. Menyhárd, *Macromolecules*, 2007, **40**, 2422.

17. M. Dong, Z. Guo, J. Yu and Z. Su, *J Polym Sci Part B: Polym Phys*, 2008, **46**,

1725.

18. M. Nie, R. Han and Q. Wang, *Ind Eng Chem Res*, 2014, **53**, 4142.

19. R. Han, Y. Li, Q. Wang and M. Nie, *RSC Adv.*, 2014, **4**, 65035.

20. R. Phillips and J.A. E. Månson, *J Polym Sci Part B: Polym Phys*, 1997, **35**, 875.

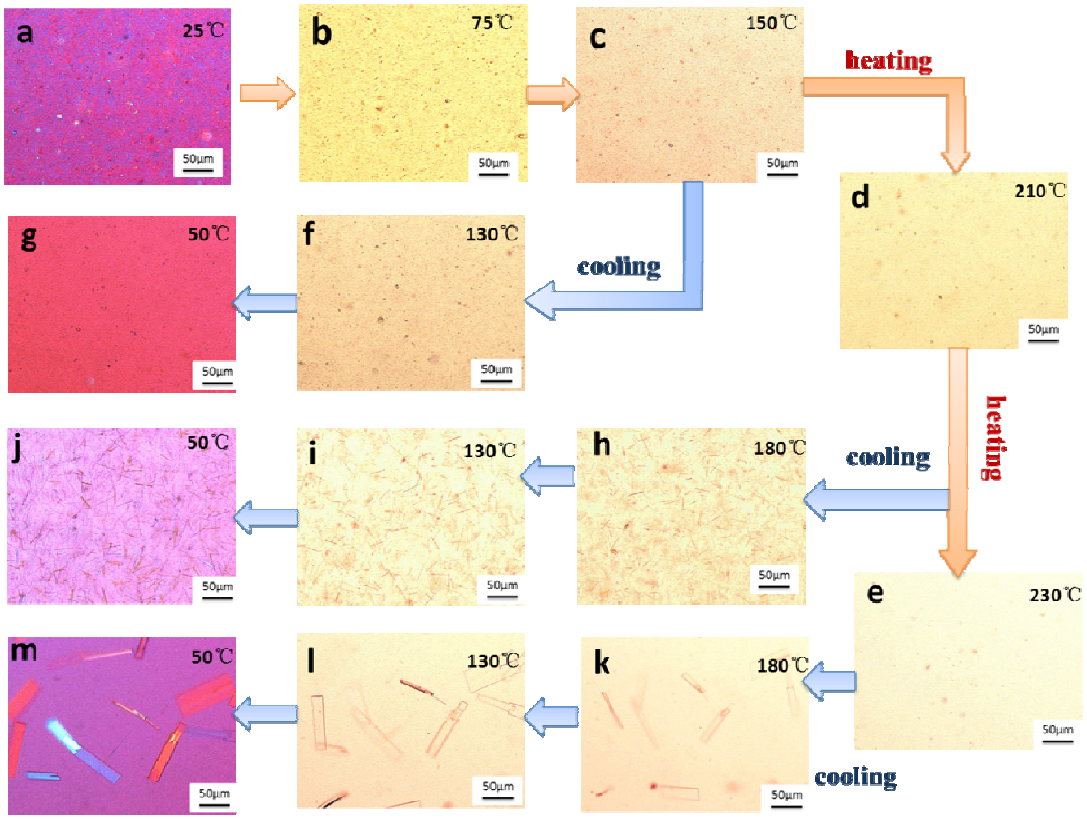


Figure 1 Optical micrographs for PCL with 0.7% NAs: (a)–(e) are heating process at a rate of 10°C/min and (f)–(m) are cooling process at a rate of 10°C/min from the different melting temperature; (f) and (g) are cooled from 150°C; (h), (i) and (j) are cooled from 210°C; (k), (m) and (l) are cooled from 230°C.

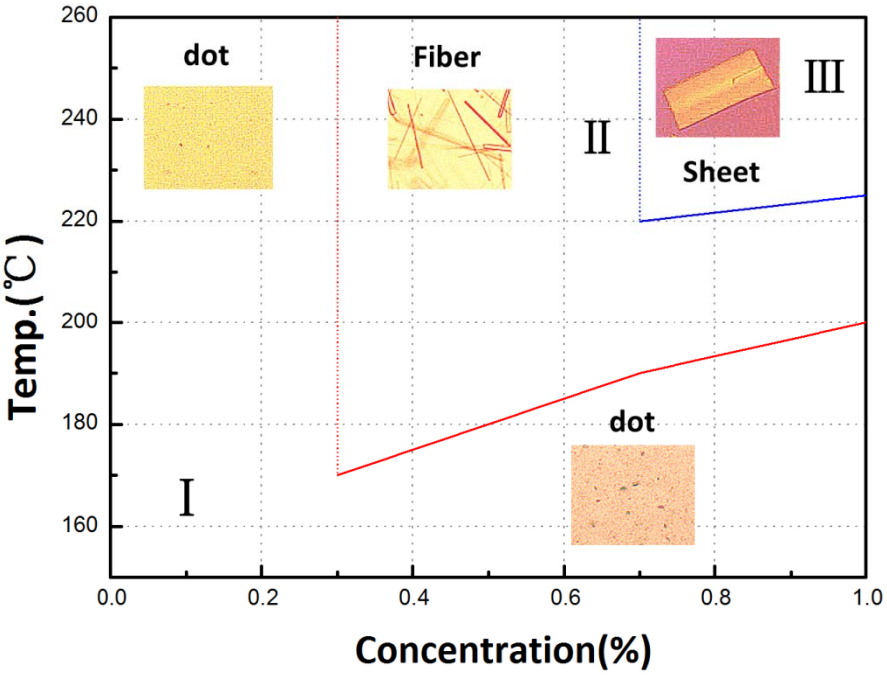


Figure 2 Morphological phase diagram of NAs in PCL melts. Red solid line represented the formed temperature of fiber NAs and blue solid line corresponded to the critical formed temperature of flake structure.

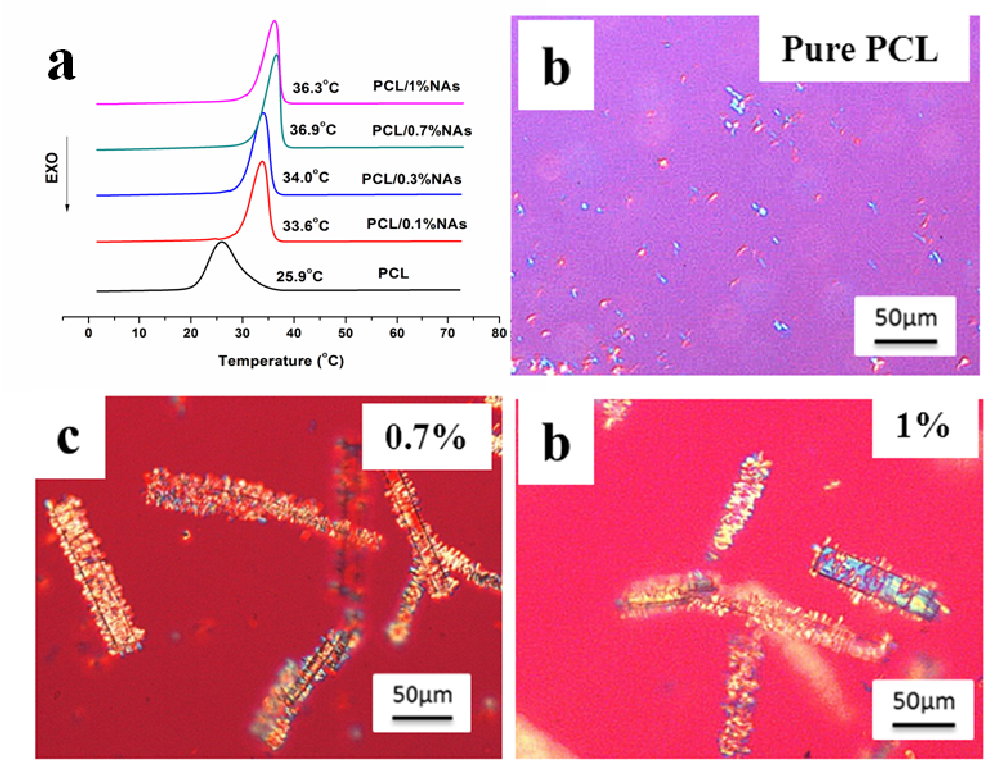


Figure 3 DSC cooling thermograms of PCL/NAs blends with the different concentration at the cooling rate of 10°C/min(a); PLM images of pure PCL(b) and PCL with 0.7%(c) and 1%(d) NAs.